

SCIENTIFIC COUNCIL MEETING - JUNE 2021

Spatial state-space survey-based stock assessment (SSURBA) model for the Grand Bank stock of American plaice

Rajeev Kumar, Divya A. Varkey, Laura Wheeland

Fisheries and Oceans Canada, Northwest Atlantic Fisheries Centre,
P.O. Box 5667, St. John's, Newfoundland, Canada A1C-5X1

Abstract

Here we updated a previously published state-space spatial survey-based stock assessment (SSURBA) model with data up to 2020 to inform spatial variation in relative stock trends of American plaice in NAFO Divisions 3LNO. The model features estimation of survey gear catchability (q) that changes spatially and temporally following changes in fish growth and survey gears. Furthermore, the model assumes natural mortality (M) is size-dependent and therefore, similar to catchability, changes with years and divisions. The original version of the model fits annual spatial (i.e. three Divisions) stock number-at-age research vessel (RV) survey indices until 2016. The purpose of this report is to present the stock trends with the addition of the most recent data for the years 2017-2020 while keeping the methods unchanged. The model suggests that the overall condition of the stock remains mostly lower than the long-term average, and average fishing mortality rates have reached levels higher than the long-term average in several years after 2010.

Introduction

This report presents the relative stock trends of American plaice in NAFO divisions 3LNO from the SSURBA model (Kumar et. al. 2020) that is updated with the recent 4 years of data.

Methods

Data

The primary data used in the model are indices of abundance from the Canadian Research Vessel (RV) Spring and autumn surveys in NAFO Divisions 3LNO and EU-Spain surveys in the NAFO Regulatory Area (NRA) of Division 3N (Fig. 1).

Model

In the report, we provide only a brief description of the model. See Kumar et. al (2020) for the model details.

Process model and components

In the cohort model (Equation 1), N number of fish of age a at the start of year y in division d and the respective per-year instantaneous rate of total mortality Z , which is the sum of natural mortality rate M and fishing mortality rate F , calculates the population in the next year

$$(1) \quad N_{a+1,y+1,d} = N_{a,y,d} \exp(-F_{a,y,d} - M_{a,y,d}), \quad a = 1, \dots, A - 1; \quad y = 1, \dots, Y; \quad d = 1, \dots, D;$$
$$N_{15^+,y,d} = (N_{15^+,y-1,d} \exp(-Z_{15^+,y-1,d}) + N_{14,y-1,d} \exp(-Z_{14,y-1,d})).$$

Recruitment (R)

The recruitment ($R_{y,d}$), which is $N_{a=1,y,d}$, is modelled by a stochastic process about a mean recruitment $\mu_{R,d}$ and a spatially correlated AR (1) deviations (Equation 2).

$$(2) \quad R_{y,d} = \mu_{R,d} \exp(\delta_{y,d}); \quad \delta_{y,d} \sim AR(1)$$

Fishing mortality rate (F)

This model assumes no commercial catch for the ages 1 to 4, so we have fixed F to be zero for these younger ages. For older ages (age ≥ 5), the logarithm of $F_{a,y,d}$ in Equation (1) follows a mixed-effects model with mean $\log(\mu_{y,d})$, within division age-year correlated random deviations $\Delta_{a,y,d}$ and between divisions correlated spatiotemporal random deviations $\lambda_{y,d}$ (Equation 3).

$$(3) \quad F_{a,y,d} = \mu_{y,d} \exp(\Delta_{a,y,d} + \lambda_{y,d}), \quad a = 5, \dots, A$$

Natural mortality rate (M)

In this work, we assume an empirical relationship between M and the weight (W) of fish based on Miller and Hyun (2017), $\ln(M) = b - 0.305\ln(W)$. We model weight as a power function of length (L) and therefore reformulate the equation for M as

$$(4) \quad M_{a,y,d} = \exp(b_d) (\alpha_d L_{a,y,d})^{-\beta_d \times 0.305},$$

where b is a scaling component, α and β are the parameters of the weight-at-length model fitted separately for each division, and the value -0.305 is an allometric scaling factor commonly used for the oceanic environments (Lorenzen 1996). The plots for the spatio-temporal changes in length-at-age (Zheng et. al 2020), length-weight relationship, and growth-based M are provided in the Appendices A-C.

Observation model and components

The model parameters are estimated by fitting the observed indices $I_{a,y,s,d}$, obtained from the Canadian spring and fall survey (s) in the NAFO Divisions 3LNO and EU-Spanish spring survey in NRA 3N, to the predicted indices $\hat{I}_{a,y,s,d}$ (Equations 4 and 5).

$$(4) \quad I_{a,y,s,d} = \hat{I}_{a,y,s,d} * \exp(\epsilon_{a,y,s,d}), \quad \epsilon_{a,y,s,d} \sim N\left(0, \begin{cases} \sigma_{11}, & \text{if age} \leq 5 \\ \sigma_{12}, & \text{if age} > 5 \end{cases}\right)$$

$$(5) \quad \hat{I}_{a,y,s,d} = \frac{q_{a,y,s,d} * N_{a,y,d} * \exp(-Z_{a,y,d} * f_s)}{SAR}, \quad SAR = \begin{cases} 1.83, & \text{if Engel trawl} \\ 1.0, & \text{otherwise} \end{cases}$$

The $\hat{I}_{a,y,s,d}$ in Equation 4 is computed by using the survey-gear catchability (q), population abundance (N), additional accounting for Z from the beginning of the year to the time of survey (f_s), and swept area ratio (SAR) of Engel to Campelen (Equation 5). Note that the EU-Spanish gear is modelled with independent catchability, and the SAR-based adjustment is only applied to the Canadian RV survey series. We model q of all the three sampling gears (g) separately as a logistic function of mean-length with logistic parameters $L95$ (length at 95% catchability) and $L50$ (length at 50% catchability) (Equation 6)

$$(6) \quad q_g = \frac{1}{1 + \exp\left(\frac{\log(19)}{L95_g - L50_g} * (L50_g - L_{c,s,d})\right)}$$

Here we only provide a very short description of the model and other components, and therefore we recommend reading Kumar et al (2020) for an in-depth model description.



Objective function

We use the TMB package (Kristensen et al. 2016) in R (R Core Team 2019) for the implementation of the models. Parameters are estimated using the maximum likelihood approach (MLE), where the $-\log$ likelihood function (objective function) is minimized using the “nlminb” optimization function of R. Recruitment deviations $\delta_{y,d}$, separable AR deviations $\Delta_{a,y,d}$, and spatial year-effects $\lambda_{y,d}$ of F are estimated as random-effect parameters (Kumar et. al 2020).

Results & Discussion

Standardized residuals from all the surveys do not show any obvious systematic patterns (Fig. 2-4). In general, the model fits the data well for all the ages across all the divisions and surveys (Fig. 5-6) except for age 1, especially in the Canadian spring survey of 3L (Fig. 5). We believe that age 1 fish are very small in spring and the index perhaps represents only the faster growing age 1 fish. The model estimates spatio-temporal catchability as a function of changes in the survey gears, survey timing, and fish growth. There is a sharp increase in catchability with change from Engel to Campelen in the Canadian RV survey gear, especially for the younger ages (Fig. 7).

We partially validate the model by comparing the relative trends of division-level and combined 3LNO reported catch with the model predictions of the same. In most of the years, the trends of the two time series are fairly similar (Fig. 8); however, the model suggests that catch (bycatch) has been higher than reported values for many years in the last decade, more prominently in Division 3N. A comparison of F-at-age patterns across the divisions shows that F was consistently high for several years in 3L before the moratorium (Fig. 9).

Biomass and spawning stock biomass (SSB) trends show that the greatest declines have occurred in 3L, followed by 3O (Fig. 10). In Division 3N, biomass and SSB increased post-moratorium and reached levels close to or above average in 2005 to 2015, following which there has been a decline to below average levels. In all divisions, recruitment levels have declined from historical highs; post-moratorium some improvements have occurred in all divisions, but levels continue to be low in all divisions (Fig. 11). Stock-productivity trends are similar in 3L and 3O, but different in 3N (Fig. 12). The SSURBA model allows us to explore the contribution of each division to the total recruitment, abundance, biomass, and SSB (Fig. 13). Throughout the time series, recruitment and abundance have been relatively high in divisions 3L and 3O. However in the post-moratorium period, Division 3N has had relatively high contribution to biomass and SSB (Fig. 13).

Retrospective patterns in spawning stock biomass estimates are small (Fig. 14). Retrospective patterns are more prominent in average F, especially for Division 3N. Note that for Division 3N, the model utilizes both the Canadian RV survey and EU-Spanish survey indices. The retrospective patterns in F are also possibly related to changes in M; this model assumes fluctuations in M that are related to fish size, however there are additional aspects of natural mortality (e.g. predation, environmental drivers) that may vary independent of fish size and are not reflected in the M assumption implemented here. Further, the retrospective patterns are more prominent in 2016 and 2017 runs likely because several surveys are missing during 2014-2017 (Rideout and Ings 2018) (Fig. 1).

Conclusion

The SSURBA provides spatial trends of relative abundance and absolute F in the NAFO Divisions 3L, 3N, and 3O, the Grand Bank stock of American plaice. The model suggests that the overall condition of the stock remains mostly lower than the long-term average, and average fishing mortality rates have reached levels higher than the long-term average in several years post 2010.



References

- Kristensen, K., Nielsen, A., Berg, C.W., Skaug, H., and Bell, B. 2016. TMB: automatic differentiation and Laplace approximation. *Journal of Statistical Software* **70**(5): 1-21.
- Kumar, R., Cadigan, N. G., Zheng, N., Varkey, D. A., and Morgan, M. J. 2020. A state-space spatial survey-based stock assessment (SSURBA) model to inform spatial variation in relative stock trends. *Can. J. Fish. Aquat. Sci.*, **77**(10), 1638-1658.
- Lorenzen, K. 1996. The relationship between body weight and natural mortality in juvenile and adult fish: a comparison of natural ecosystems and aquaculture. *Journal of fish biology* **49**(4): 627-642.
- Miller, T.J., and Hyun, S.-Y. 2017. Evaluating evidence for alternative natural mortality and process error assumptions using a state-space, age-structured assessment model. *Can. J. Fish. Aquat. Sci.* **75**(5): 691-703.
- R Core Team. 2019. R: A language and environment for statistical computing. R Foundation for Statistical Computing, Vienna, Austria.
- Rideout, R.M. and D.W. Ings. 2018. Temporal And Spatial Coverage Of Canadian (Newfoundland And Labrador Region) Spring And Autumn Multi-Species RV Bottom Trawl Surveys, With An Emphasis On Surveys Conducted In 2017. NAFO SCR Doc. No 18/07.
- Zheng, N., Cadigan, N. and Morgan, M.J., 2020. A spatiotemporal Richards–Schnute growth model and its estimation when data are collected through length-stratified sampling. *Environmental and Ecological Statistics*, **27**(3), pp.415-446



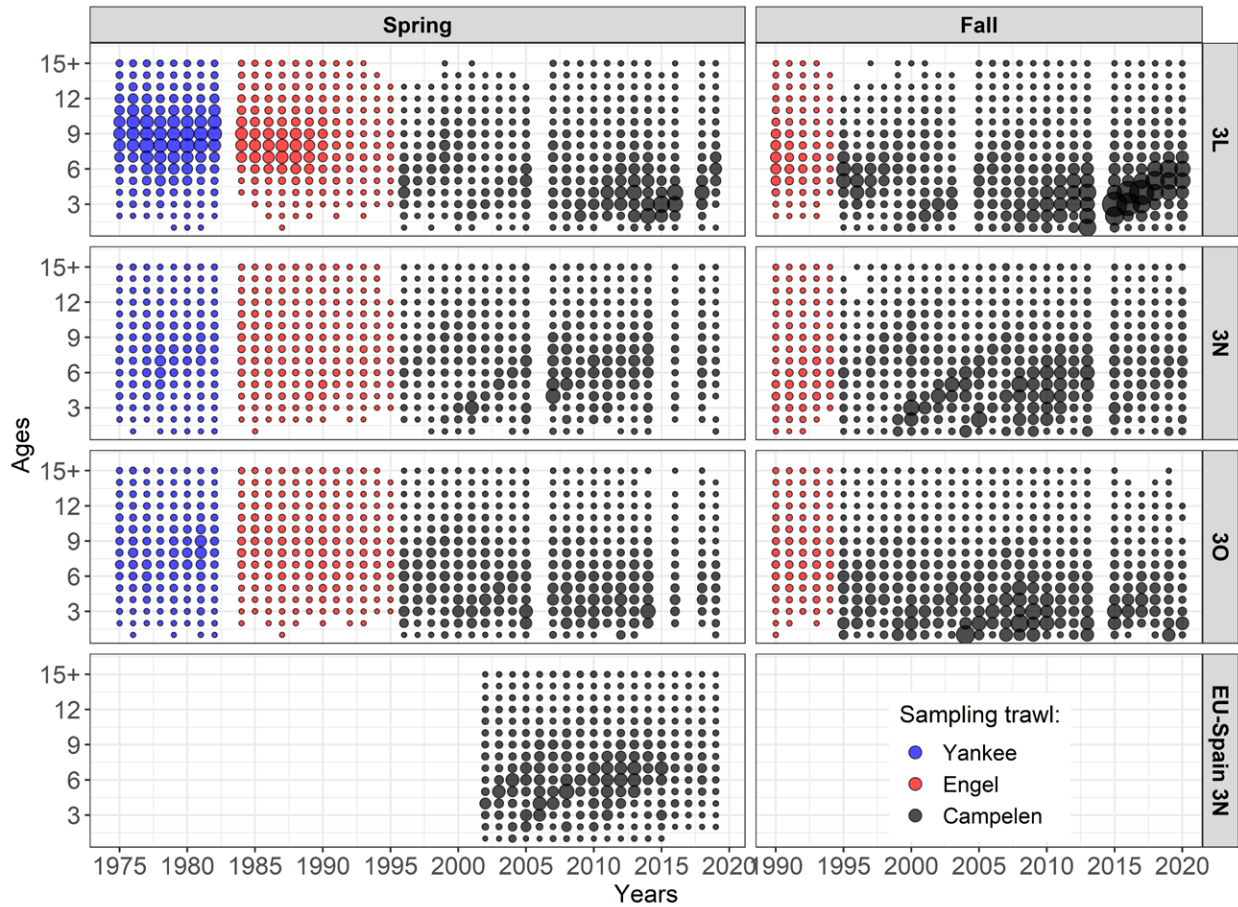


Figure 1. Spatio-temporal coverage of the Canadian and EU-Spanish survey indices used in the model.

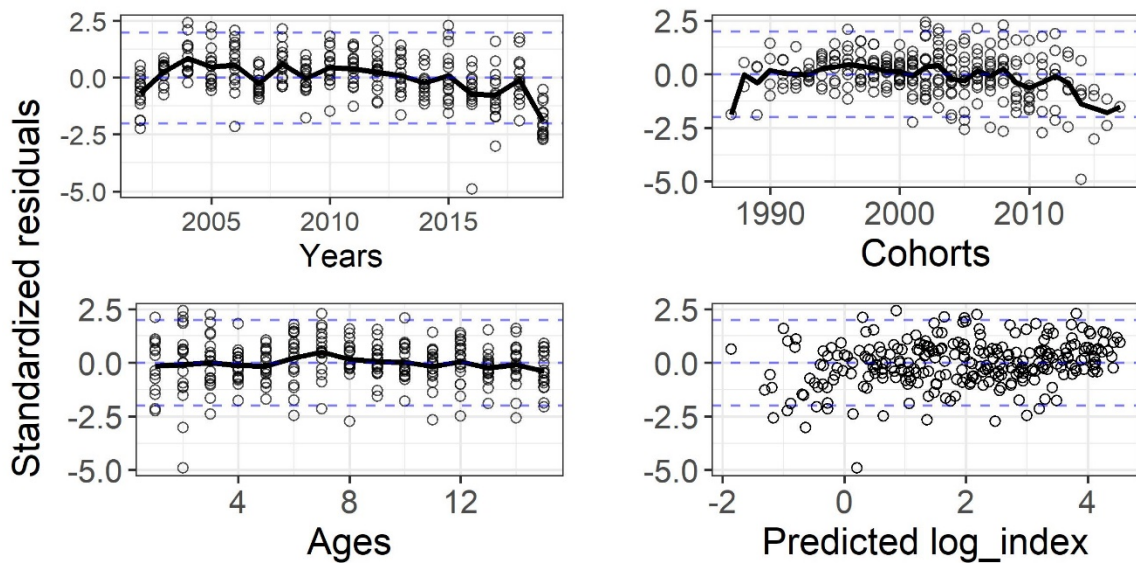


Figure 2. Standardized residuals indices obtained from the EU-Spanish RV survey are plotted against year, cohort, age, and predicted log-index for the NRA 3N.

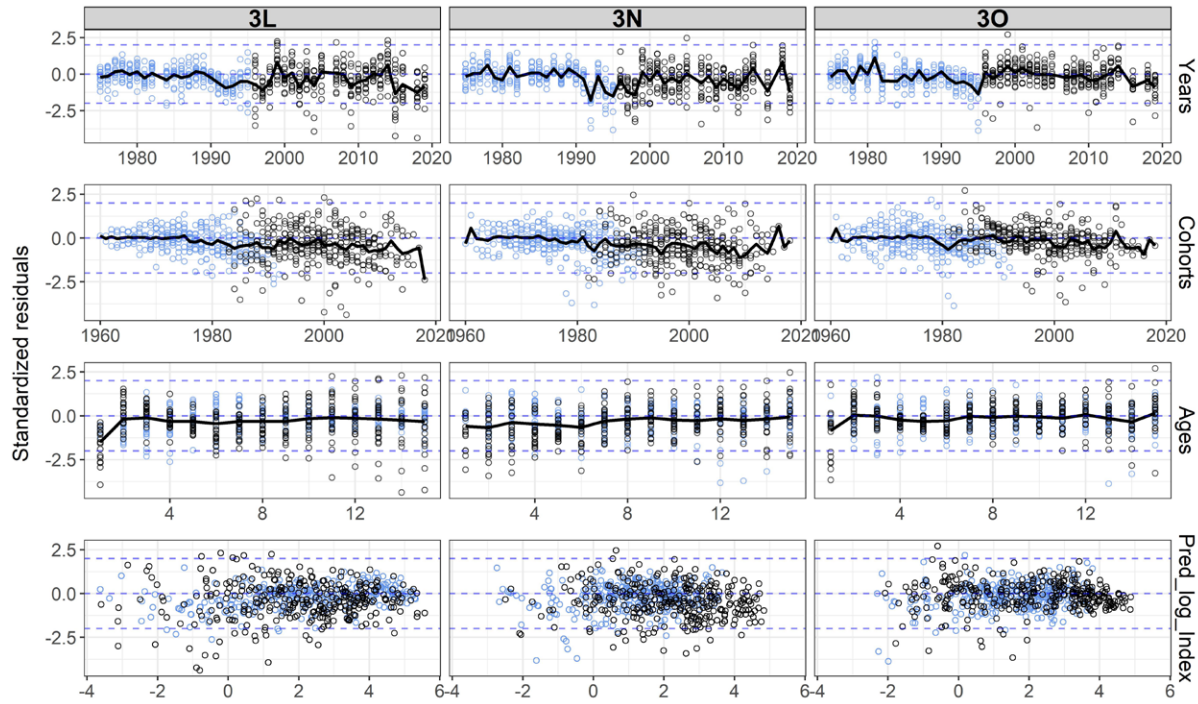


Figure 3. Standardized residuals indices obtained from the Canadian Spring RV survey are plotted against year, cohort, age, and predicted log-index for the three divisions. Residuals for Engel indices are shown in blue.

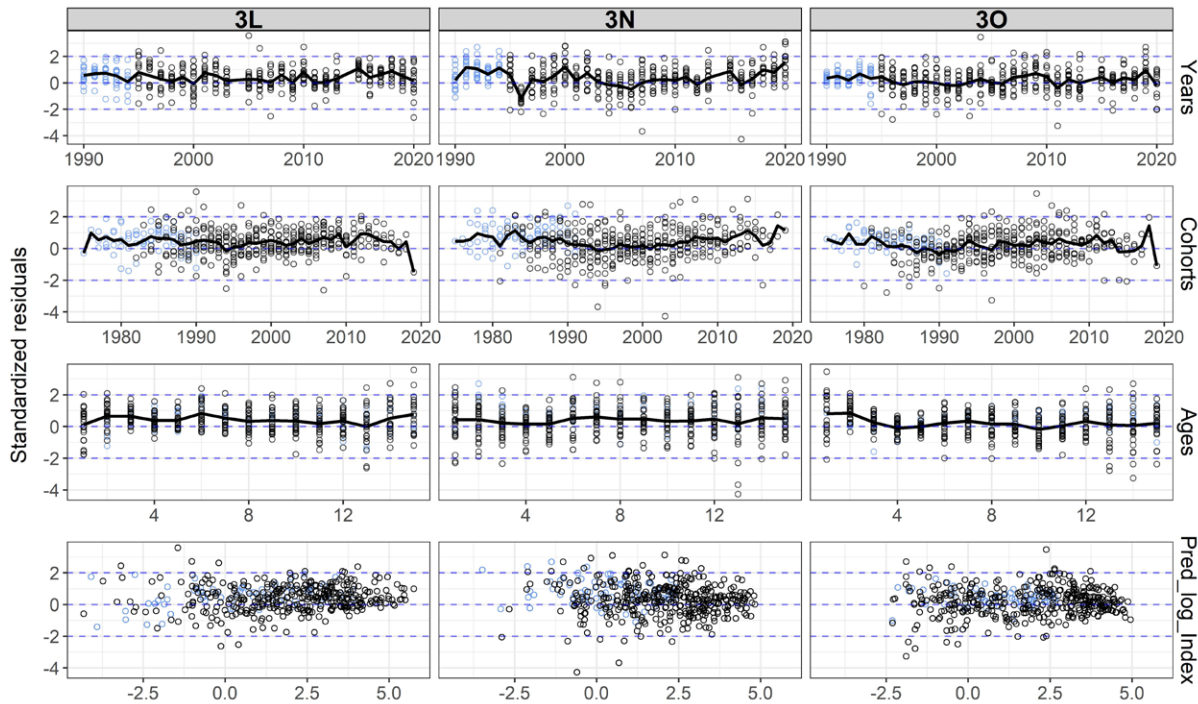


Figure 4. Standardized residuals indices obtained from the Canadian Fall RV survey are plotted against year, cohort, age, and predicted log-index for the three divisions. Residuals for Engel indices are shown in blue.

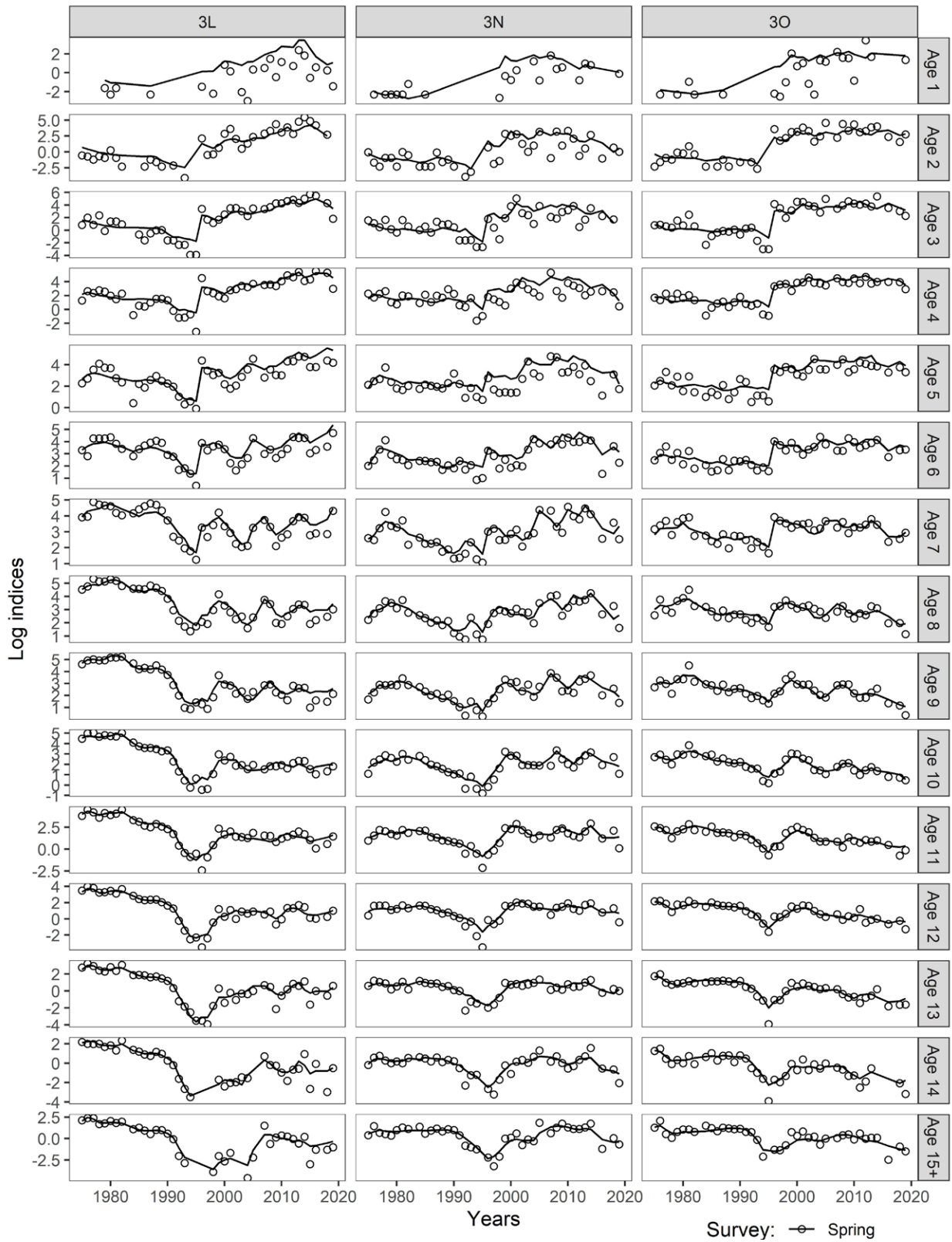


Figure 5. Model fitting to the time-series of the Canadian spring indices for the three divisions across each age.

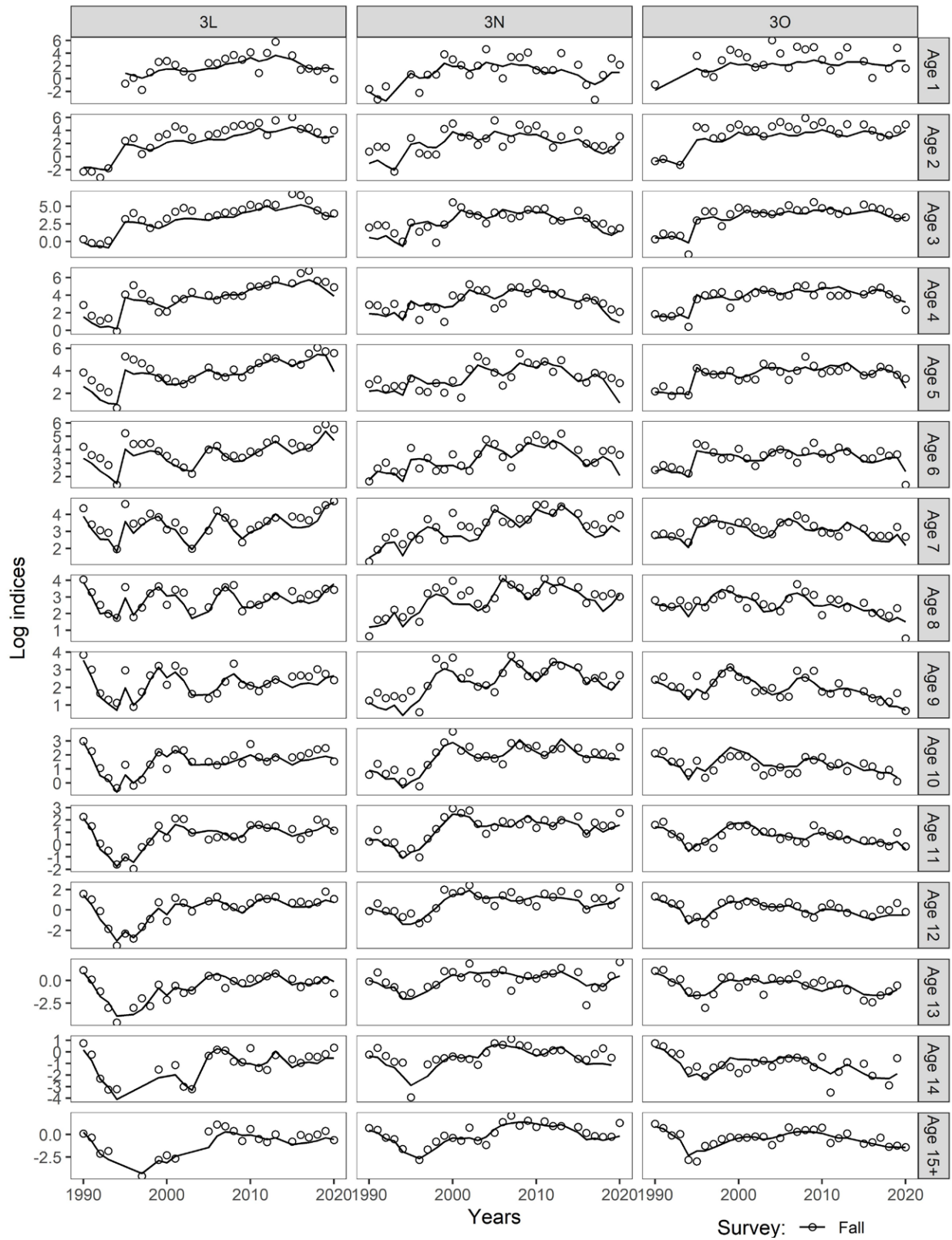


Figure 6. Model fitting to the time-series of the Canadian fall indices for the three divisions across each age.

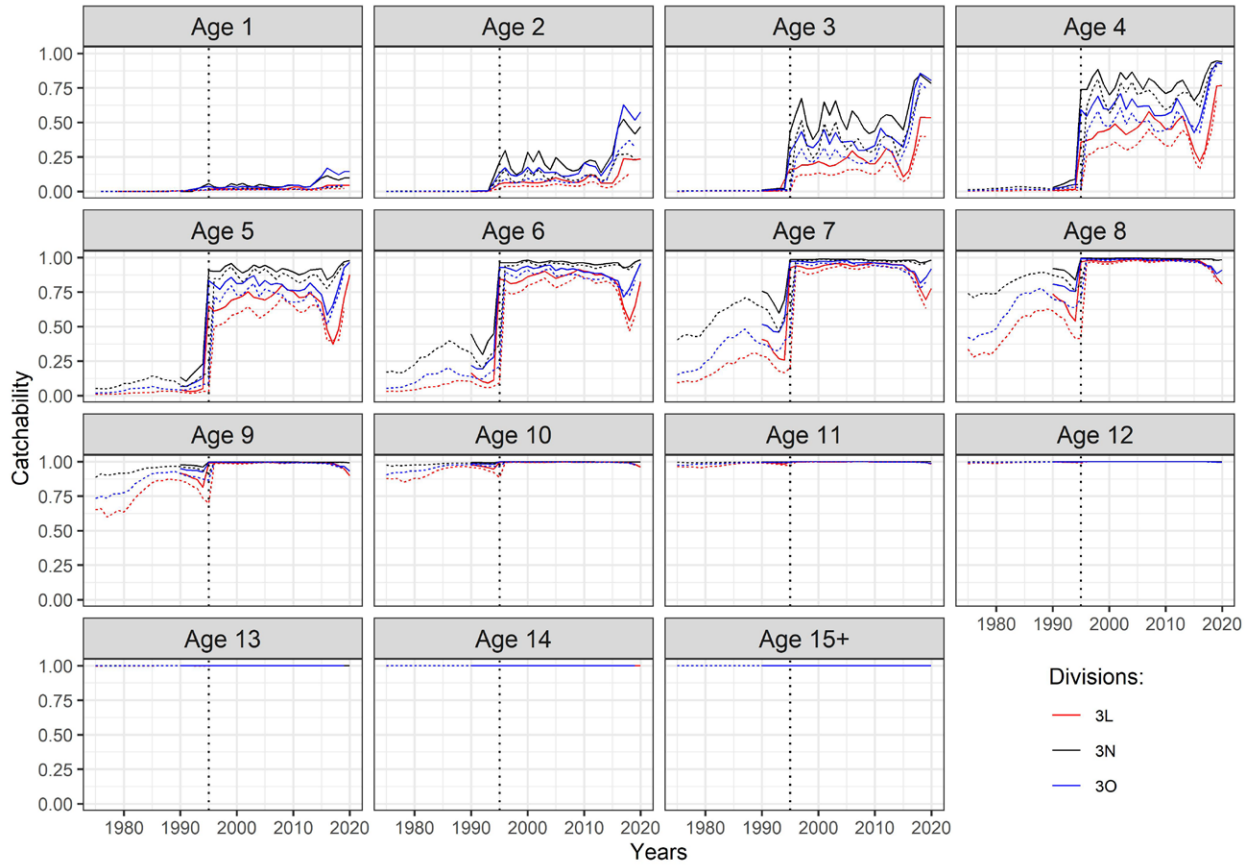


Figure 7. Spatio-temporal changes in the Canadian RV survey gear catchability.

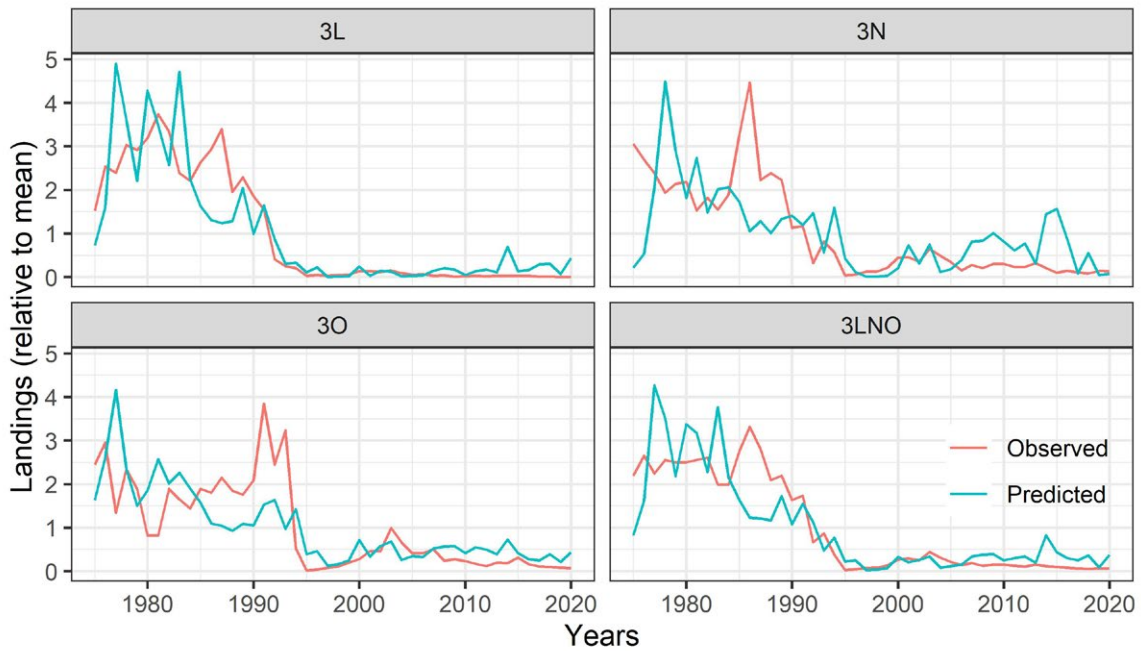


Figure 8. Plot showing relative trends of model prediction of landings and reported catch in the Divisions 3L, 3N, 3O and combined 3LNO.



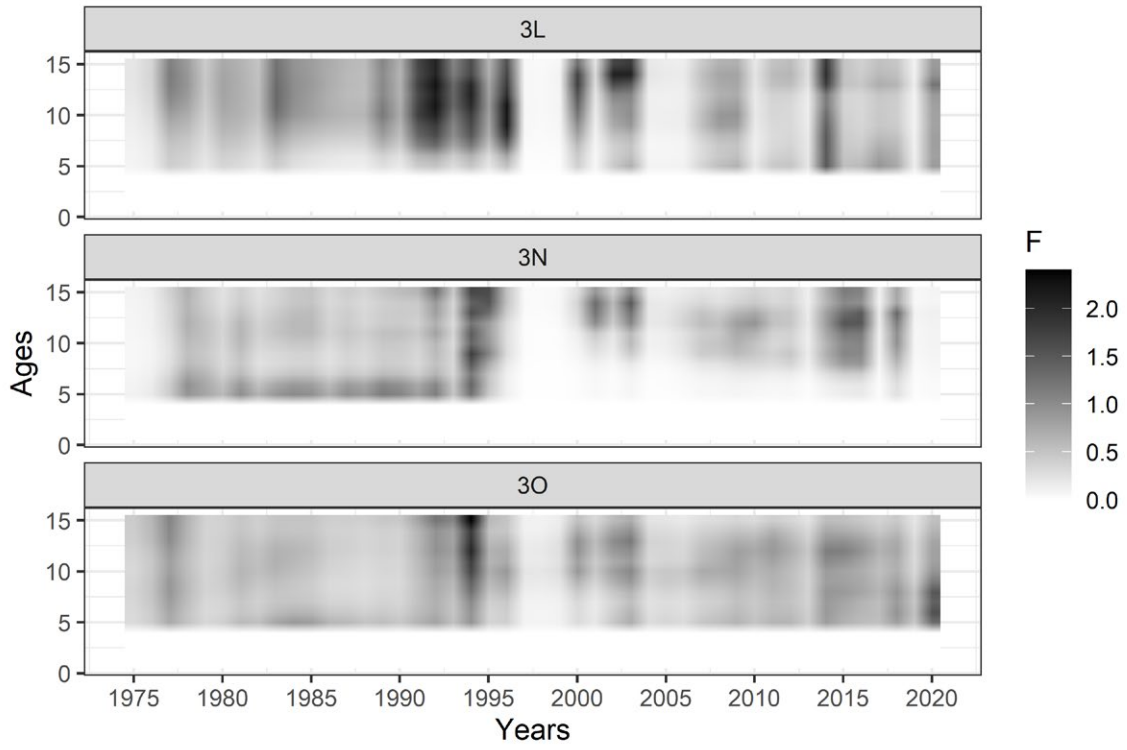


Figure 9. Raster plot showing age-wise instantaneous rate of fishing mortality (F) in the three Divisions.

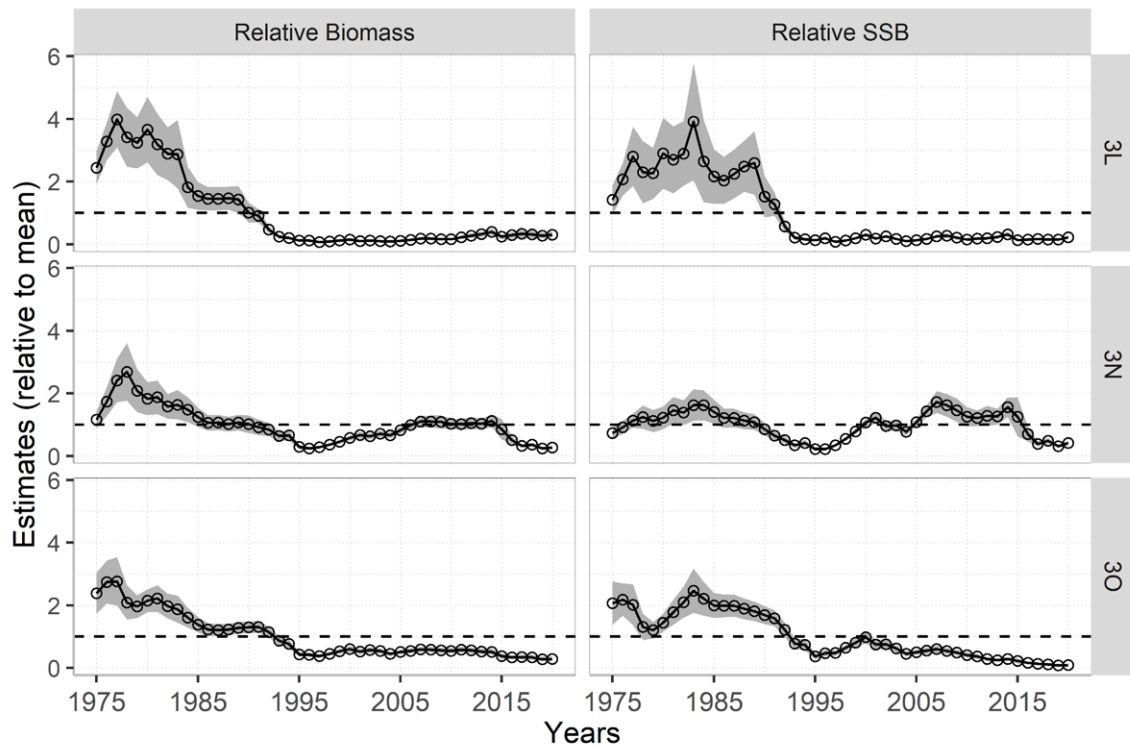


Figure 10. Relative estimate of biomass and SSB in the three NAFO divisions with the shading of 95% confidence interval.



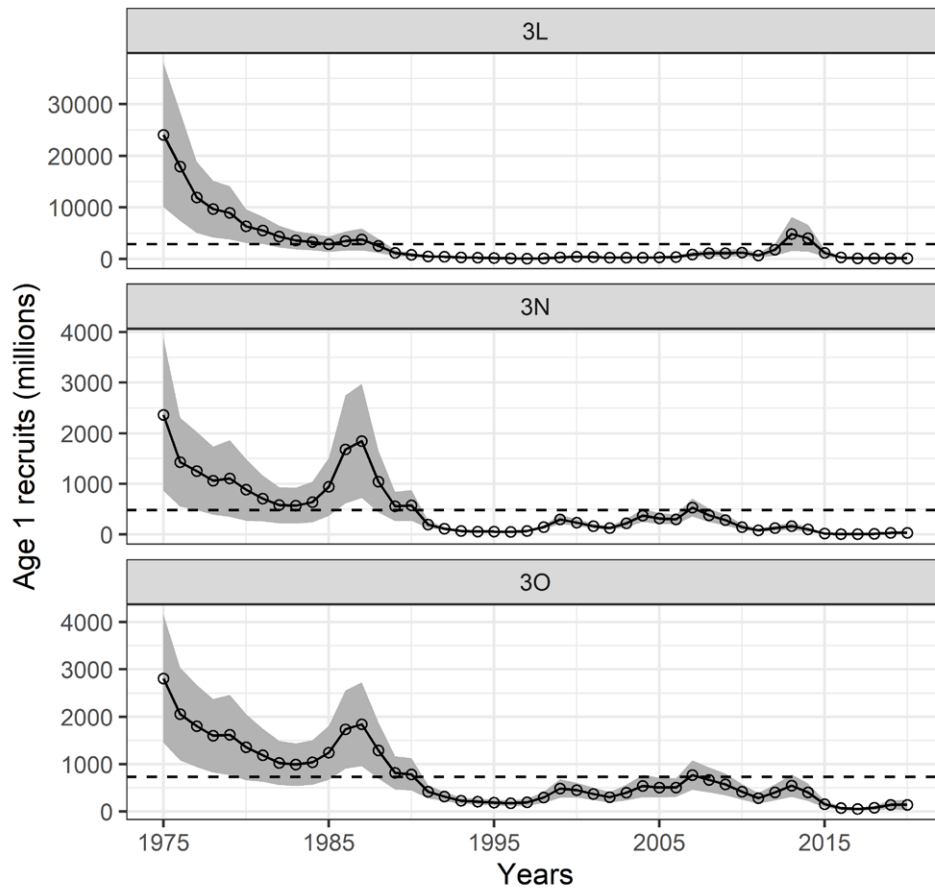


Figure 11. Relative recruitment of age 1 in the three NAFO divisions with the shading of 95% confidence interval.

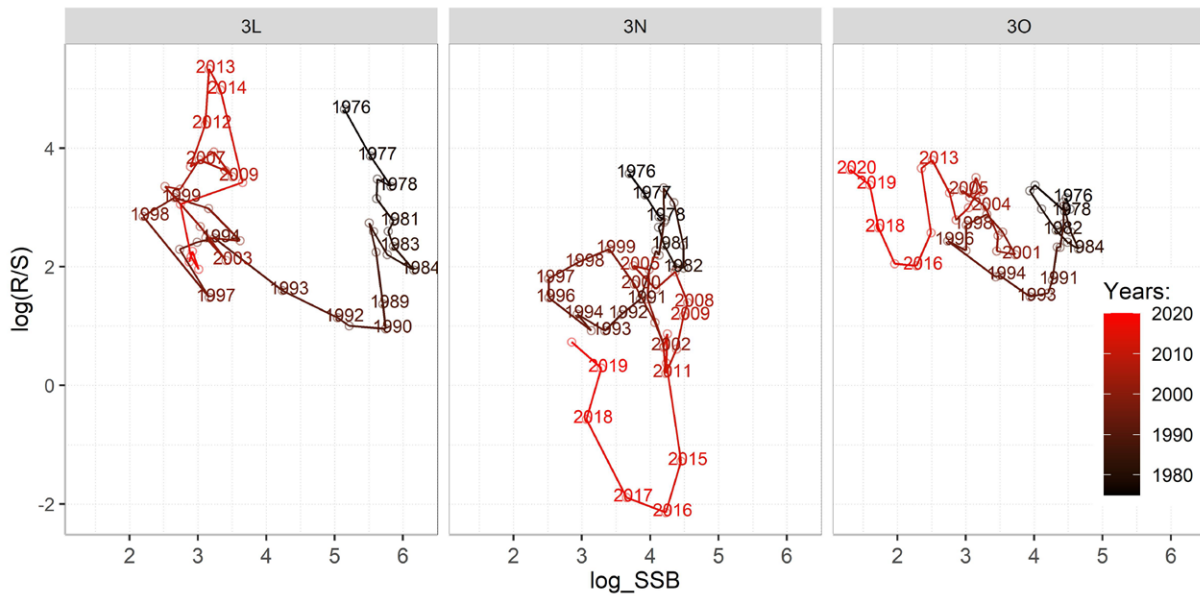


Figure 12. Log of Recruit-per Spawner (R/S) plot showing temporal variation in the productivity.



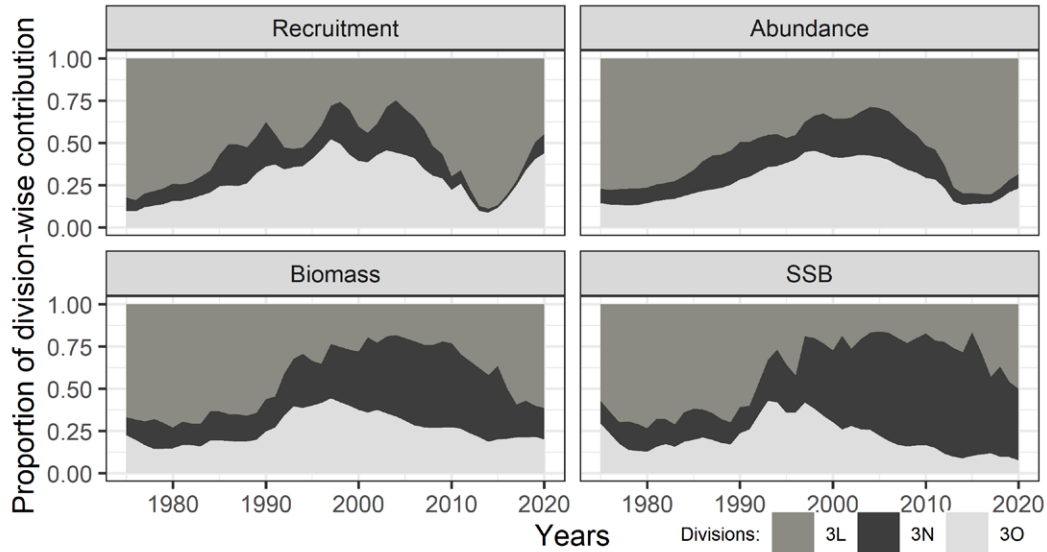


Figure 13. Temporal changes in the relative contribution of the three divisions in the total stock recruitment, abundance, biomass, and SSB.

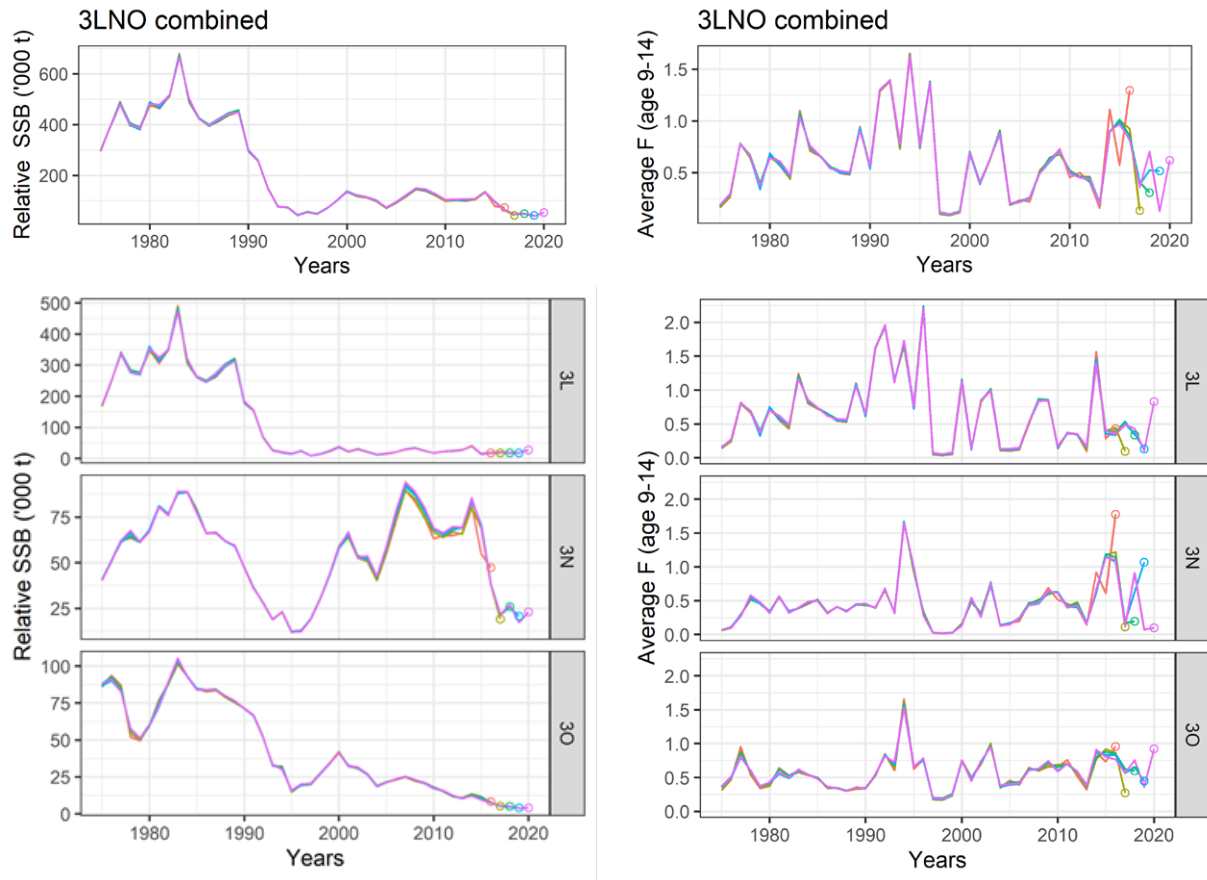
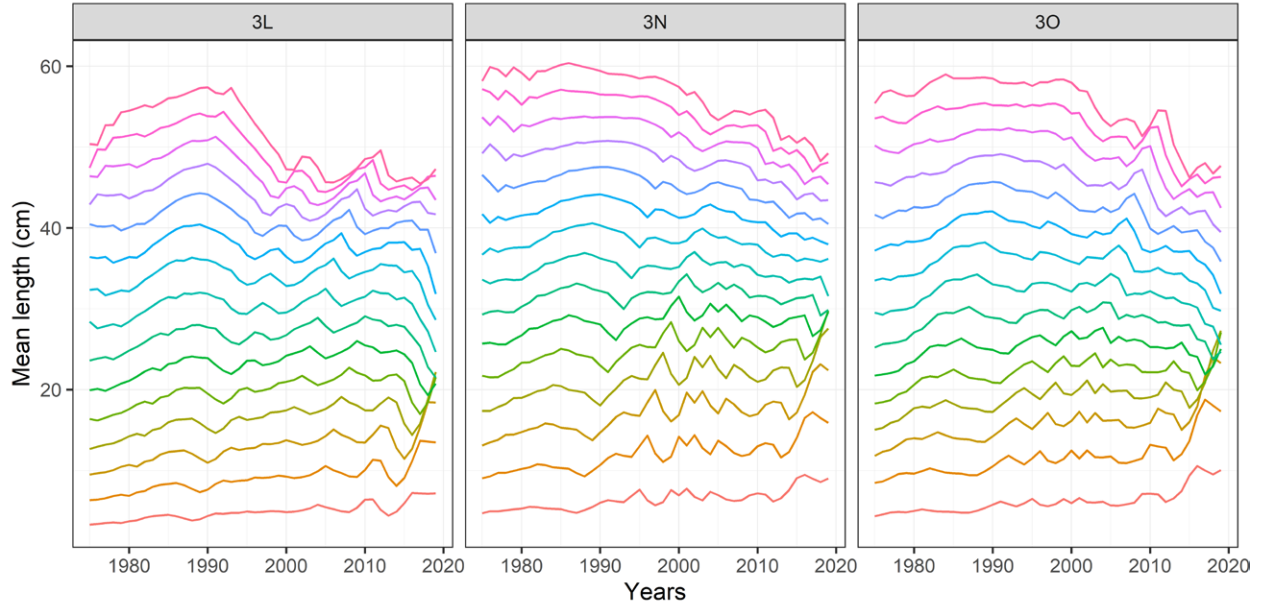


Figure 14. Spatial retrospective analysis shows the changes in relative SSB and F in Division 3L, 3N, 3O and combined 3LNO with each additional year of data used from 2016 to 2020. Circles mark the corresponding retrospective years.

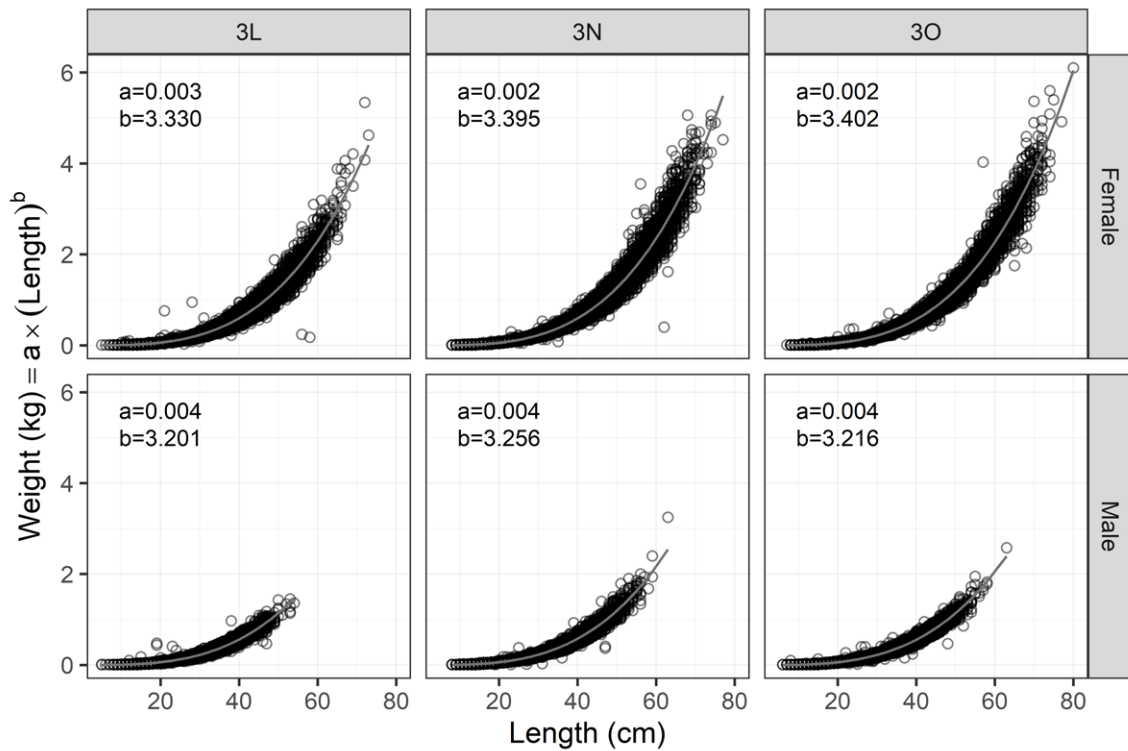


Appendix A: Length-at-age

Spatio-temporal changes in the mean length at age (age 1-15+) from Zheng et. al (2020).



Appendix B: Length-weight relationship



Appendix C: Natural mortality M

Estimation of M based on Lorenzen (1996) and Miller and Hyun (2017) formulation.

